Conformational Studies of Phenyl- and (1-Pyrenyl)triarylmethylcarbenium Ions: Semiempirical Calculations and NMR Investigations under Stable Ion Conditions

Poul Erik Hansen,* Jens Spanget-Larsen, and Kenneth K. Laali

Department of Life Sciences and Chemistry, Roskilde University, P.O. Box 260, DK-4000 Roskilde, Denmark, and Department of Chemistry, Kent State University, Kent, Ohio 44242-0001

Received August 19, 1997

Highly stable crowded carbenium ions such as (1-pyrenyl)diphenylmethylcarbenium ion (**2**) and 1,6- (**3**) and 1,8-bis(diphenylmethylenium)pyrene [dication] (**4**) and their dibrominated analogues (**3Br** and **4Br**) have been studied at low and at ambient temperatures. **2** shows a conventional two-ring flip (*ph*,*ph*), whereas the disubstituted pyrene derivatives show one-ring flips (*py*) and two-ring flips (*ph*,*ph*) with a higher rotational barrier in agreement with AM1 calculations. A series of calculations show that the AM1 method gives the transition-state energies in best agreement with experiment. The propeller-shaped geometry of these molecules is reflected in characteristic low-frequency resonances of the phenyl rings. At low temperature, **3** and **4** exist as rotational isomers with C_2 and C_s (or C_i) symmetry. In **4**, steric interaction makes the two rotamers slightly different in energy (1 kcal). For **4** or **4Br**, the ^{13}C chemical shift differences between the C_2 and the C_s species of **4** or **4Br** correlate roughly with the calculated charge differences between the C_2 and the C_s species. The charge at the C^+ carbon is most extensively delocalized in **2**, whereas in **3** and **4** with two C^+ groups the pyrene moieties are less effective in charge delocalization.

Introduction

Several classes of sterically crowded triarylcarbenium ions are known. Now a textbook example, triphenylmethyl (trityl) cation, is probably the most thoroughly studied member and the first long-lived carbocation to be studied.[1,2] The importance of quinoidal resonance contributors in trityl cation and its propeller-shaped structure are well established.[3]

In comparison, the PAH-substituted carbenium ion analogues and the mode of charge delocalization in such species are not as well studied, except for triazulenylmethyl cations whose dynamics have been a subject of intense recent work by the Asao group.[4−6]

Carbenium ions α to PAHs are interesting models of PAH epoxide ring opening en route to PAH−DNA adduct formation.[7−9]

Their charge delocalization mode(s) and dynamics are, therefore, important in relation to mechanistic carcinogenesis and PAH activation by electrophilic pathways.

The present paper deals with generation, dynamic NMR, and semiempirical calculations (MMX,[10] AM1,[11] PM3,[12] MNDO,[13] MINDO/3[14]) on (1-pyrenyl)diphenylmethyl cations. Since there is no degeneracy in these carbenium ions, flipping of the rings can be followed by DNMR; the rotational patterns can be determinants in the stability and reactivity of these ions.

Our computational studies began with the trityl cation for which the X-ray structure is known;[3] elegant dynamic NMR studies on substituted trityl cations are also available.[15,16]

By use of semiempirical MO and force field calculations, the minimum energy conformations of trityl cation and the preferred ring rotations were evaluated and compared with experiment. Subsequently, the conformations and the charge distribution pattern in the more crowded (1-pyrenyl)diphenylmethyl cations and their related dications (see Figure 1) were probed along with DNMR studies of the persistent ions.

Results

Theoretical Studies. To gain some insight into the factors influencing conformational interconversion processes, their activation enthalpies were studied by a

* To whom correspondence should be addressed. Tel.: +45 46742432. Fax: +45 46743011. E-mail: POULERIK@virgil.ruc.dk.

(1) *Carbonium Ions*, Bethell, D., Gold, V., Eds.; Academic Press: London, 1967.
(2) *Superacids*; Olah, G. A., Prakash, G. K. S., Sommer, J.; J. Wiley: New York, 1985.
(3) Gomes de Mesquita, A. H.; MacGilvary, C. H.; Eriks, K. *Acta Crystallogr.* **1965**, *18*, 437.
(4) Ito, S.; Fujita, M.; Morita, N.; Asao, T. *Chem. Lett.* **1995**, 475.
(5) Ito, S.; Morita, N.; Asao, T. *Bull. Chem. Soc. Jpn.* **1995**, *68*, 2011.
(6) Ito, S.; Morita, N.; Asao, T. *Bull. Chem. Soc. Jpn.* **1995**, *68*, 1409.
(7) Nashed, N. T.; Rao, T. V. S.; Jerina, D. M. *J. Org. Chem.* **1993**, *58*, 6344.
(8) Nashed, N. T.; Bax, A.; Loncharich, R. J.; Sayer, J. M.; Jerina, D. M. *J. Am. Chem. Soc.* **1993**, *115*, 1711.
(9) Nashed, N. T.; Sayer, J. M.; Jerina, D. M. *J. Am. Chem. Soc.* **1993**, *115*, 1723.
(10) Gajewski, J. J.; Gilbert, K. E.; McKeIvey, J. *Adv. Mol. Model.* **1990**, *2*, 65.
(11) (a) Dewar, M. J. S.; Zoebisch, E. G.; Healy, E. F.; Stewart, J. J. P., *J. Am. Chem. Soc.* **1985**, *107*, 3902. (b) Dewar, M. J. S.; Zoebisch, E. G. *THEOCHEM* **1988**, *49*, 1.
(12) Stewart, J. J. P. *J. Comput. Chem.* **1989**, *10*, 209, 221; **1990**, *11*, 543.
(13) (a) Dewar, M. J. S.; Thiel, W. *J. Am. Chem. Soc.* **1977**, *99*, 4899, 4907. (b) Dewar, M. J. S.; McKee, M. L. *J. Am. Chem. Soc.* **1977**, *99*, 5231. (c) Dewar, M. J. S.; Rzepa, H. S. *J. Am. Chem. Soc.* **1978**, *100*, 58, 777, 784.
(14) (a) Bingham, R. C.; Dewar, M. J. S.; Lo, D. H. *J. Am. Chem. Soc.* **1975**, *97*, 1285, 1294, 1302, 1307. (b) Dewar, M. J. S. *Science* **1975**, *187*, 1037.
(15) Schuster, I. I.; Colter, A. K.; Kurland, R. J. *J. Am. Chem. Soc.* **1968**, *90*, 4679.
(16) Rakshys, J. W., Jr.; McKinley, S. V.; Freedman, H. H. *J. Am. Chem. Soc.* **1970**, *92*, 3518; **1971**, *93*, 6522.

S0022-3263(97)01548-X CCC: $15.00 © 1998 American Chemical Society
Published on Web 02/20/1998

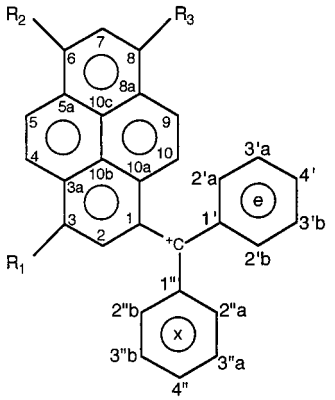

2	$R_1 = R_2 = R_3 = H$	
3	$R_1 = R_3 = H$	$R_2 = {}^+C(Ph)_2$
3Br	$R_1 = R_1 = Br$	$R_3 = {}^+C(Ph)_2$
4	$R_1 = R_2 = H$	
4Br	$R_1 = R_2 = Br$	$R_3 = {}^+C(Ph)_2$

Figure 1. Numbering of molecules. The endo ring (e) atoms are marked with a prime and the exo ring (x) atoms with a double prime.

number of theoretical procedures. Entropy effects were not considered, and the cations **1**−**4** were treated as free, unsolvated species. Solvent effects and effects due to complex formation with counterions are thus neglected. Interpretation of the present results should be made with due caution, particularly for the doubly charged species **3** and **4**.

The conformational transition-state (TS) structures were generally estimated by the assumption of idealized geometries: The flipping rings were fixed in conformations perpendicular to the plane of the cation center, and the remaining rings were kept coplanar with this plane. All other geometrical parameters were optimized by the respective calculational methods. The energy gradients obtained for the idealized TS structures were in all cases close to zero (single-point calculations without restraints), consistent with the assumption that the structures correspond to saddle points on the potential energy hypersurface. The individual TSs are identified by indication of the rings involved in the flipping process; e.g., the notation (*ph*,*ph*) refers to a TS where two phenyl rings are perpendicular to and the remaining ring coplanar with the plane of the cation center.

The Trityl Cation (1). Several calculational procedures were tested for their ability to reproduce the available experimental results for the trityl cation, 1. The methods applied were the MMX molecular mechanics method[10] and the semiempirical MO procedures AM1,[11] PM3,[12] MNDO,[13] and MINDO/3,[14] using commercially available software.[17,18] The predicted conformational activation enthalpies for one-ring (*ph*), two-ring (*ph*,*ph*), and three-ring (*ph*,*ph*,*ph*) flip in **1** are given in Table 1. The results diverge considerably; the AM1 and MMX results seem most consistent with the experimental evidence:[15,16] They favor the two-ring flip process (*ph*,*ph*) and predict an activation enthalpy reasonably close to the experimental estimate of 9 kcal/mol (1 kcal = 4.184 kJ). The TS structures predicted by AM1 are indicated in Figure 2. This method predicts that the two-ring process is favored over the one-ring process by about 1 kcal/mol; in the case of PM3, this situation is reversed. MNDO and MINDO/3 predict relatively low activation energies, apparently as the result of a different balance between steric and conjugative effects; steric effects are "harder" in these methods, compared to the later developments AM1 and PM3.[11−14] In the following, we shall refrain from further application of the MNDO and MINDO/3 methods.

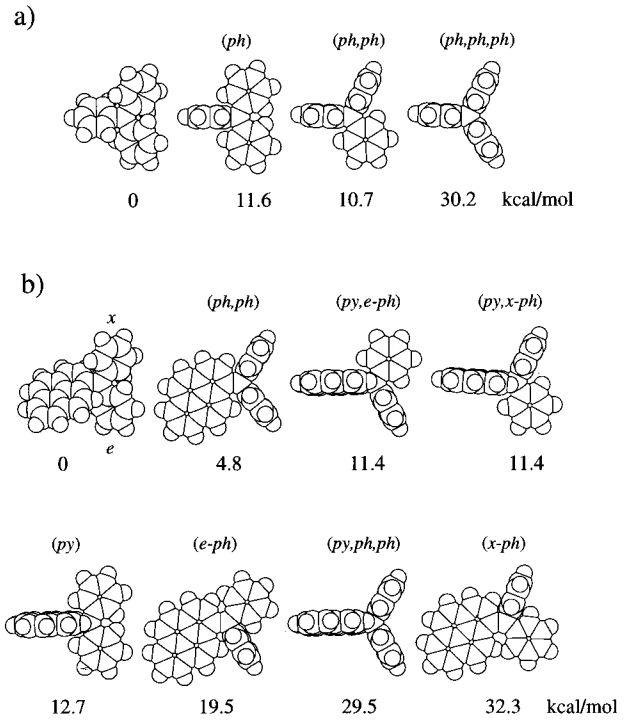

Figure 2. AM1 ground-state structure and different transition states corresponding to one-ring, two-ring, and three-ring flip for (a) the trityl cation **1** and (b) the (1-pyrenyl)diphenylmethyl cation **2**, with indication of the predicted activation enthalpies (kcal/mol).

Table 1. Calculated Activation Enthalpies (kcal/mol) for Conformational Interconversion in the Trityl Cation (1)

	one-ring flip (*ph*)	two-ring flip (*ph*,*ph*)	three-ring flip(*ph*,*ph*,*ph*)
AM1	11.6	10.7	30.2
PM3	6.6	7.9	26.1
MNDO	13.0	4.2	19.0
MINDO/3	9.4	1.4	6.2
MMX	18.1	10.7	23.8

The (1-Pyrenyl)diphenylmethyl Cation (2). Calculations on **2** were performed with AM1, PM3, and MMX. Under the present assumptions of idealized TS structures (see above), the TSs for two-ring flip (*py*,*ph*) involving the *py* (1-pyrenyl) group and one of the phenyl groups have the same activation energy, irrespective of whether it is the e-*ph* (*endo*-phenyl) or x-*ph* (*exo*-phenyl) ring that is involved in the process. The predicted activation enthalphies are given in Table 2, and TS structures computed with AM1 are indicated in Figure 2. In the case of MMX, it was not possible to compute TS structures corresponding to e-*ph* or x-*ph* one-ring flipping; these structures where the *py* group is coplanar with one of the *ph* groups are highly hindered (see Figure 2).

(17) PCMODEL for Windows; Serena Software, 1993, Box 3076, Bloomington, IN 47402-3076.

(18) HyperChem for Windows, Release 4.5, 1995, Hypercube, Inc., 419 Philip St., Waterloo, Ontario, Canada N2L 3X2.

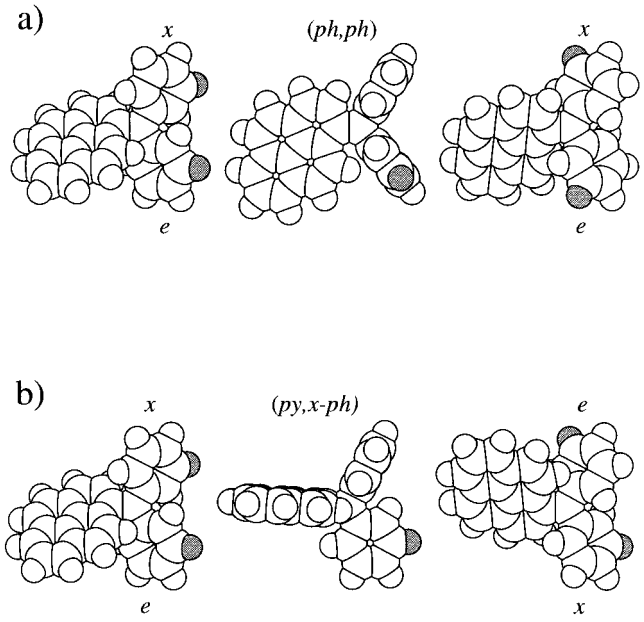

Figure 3. AM1 structures of initial ground state, transition state, and the product ground state of (a) two-ring (*ph*,*ph*) flip and (b) two-ring (*py*,x-*ph*) flip in the (1-pyrenyl)diphenylmethyl cation **2**. Since flipping of the 1-pyrenyl group is not involved in the (*ph*,*ph*) process, the *endo*-phenyl remains endo, and the *exo*-phenyl remains exo; equivalent positions within each phenyl group are equilibrated (as exemplified by the marked hydrogen atoms) but positions on different phenyl groups are not. The (*py*,x-*ph*) process involves pyrenyl flipping, and the *exo*-phenyl is transformed into endo and vice versa; in combination with the corresponding (*py*,e-*ph*) process (Figure 2) all equivalent positions on the two phenyls are equilibrated.

Table 2. Calculated Activation Enthalpies (kcal/mol) for Conformational Interconversions in the (1-Pyrenyl)diphenylmethyl Cation (2)

	one-ring flips			two-ring flips		three-ring flip
	(*py*)	(*e*-*ph*)	(*x*-*ph*)	(*py*,*ph*)	(*ph*,*ph*)	(*py*,*ph*,*ph*)
AM1	12.7	19.5	32.3	11.4	4.8	29.5
PM3	8.2	13.2	25.2	8.7	1.5	24.5
MMX	21.7			8.8	10.8	18.0

AM1 and PM3 clearly predict that two-ring (*ph*,*ph*) flipping requires the lowest activation enthalpy for **2**. The computed TS for this process is stabilized by 4−6 kcal/mol relative to the corresponding process in **1** (Table 1). This is easily explained by the greater conjugative effect of the pyrene π-system that becomes coplanar with the C+ center during the (*ph*,*ph*) process in the case of **2** (Figure 2). According to AM1, the formal net charge of the cation center is reduced from +0.385 in the (*ph*,*ph*) TS of **1** to +0.244 in the corresponding TS of **2**, indicating the increased delocalization of the positive charge. However, the MMX results do not agree with this trend. The MMX force field includes an SCF treatment of the π-system, but inspection of MMX charge distributions indicates that the method hardly distinguishes between the conjugative effects of a phenyl group and a 1-pyrenyl group. The MMX method thus tends to underestimate the conjugative stabilization of the TS correponding to two-ring (*ph*,*ph*) flipping in **2**.

The second lowest TS energy is predicted by AM1 and PM3 to correspond to two-ring (*py*,*ph*) or one-ring (*py*). Both of these processes involve flipping of the 1-pyrenyl group, and their TSs are predicted to be fairly close in energy and 6−7 kcal/mol above the lowest TS corresponding to two-ring (*ph*,*ph*). Hence, according to AM1 and PM3, the lowest TS of **2** corresponds to two-ring (*ph*,*ph*) where *py* does not flip, well separated from higher TSs with *py* flipping. This prediction is possibly significant: The two-ring (*ph*,*ph*) flip does not equilibrate different *ph* group positions (endo remains endo, and exo remains exo) but equilibrates the two ortho and the two meta positions on each *ph* group; see Figure 3. Equilibration of endo and exo *ph* requires *py* flip, see Figure 3, but this requires additional energy. AM1 computes activation enthalpies close to 5 and 11 kcal/mol for the two processes; according to this prediction, it should be possible to observe the two different equilibration processes by variable-temperature NMR.

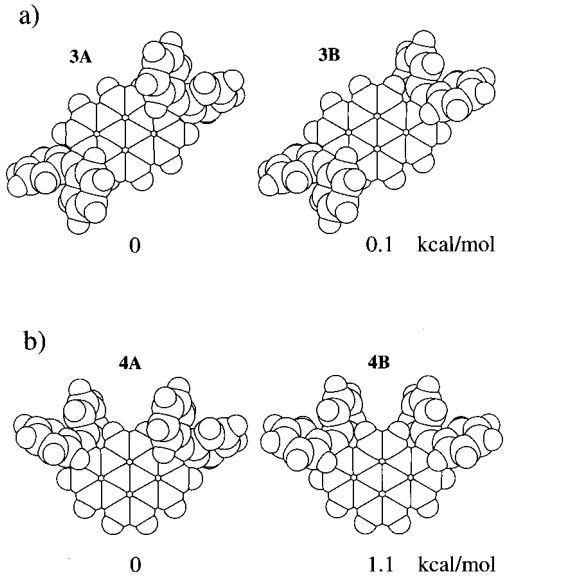

Figure 4. AM1 structures for stable conformers of the 1,6- and 1,8-bis(diphenylmethylenium) pyrene dications **3** and **4** (relative energies in kcal/mol). The molecular symmetry is C_2 for **3A** and **4A**, C_i for **3B**, and C_s for **4B**.

Table 3. Relative AM1 Enthalpies (kcal/mol) for Conformers of the 1,6- and 1,8-Bis(diphenylmethylenium)Pyrene Dications (3 and 4) and for Low-Energy Interconversional Model Transition States[a]

	2	3	4
conformer **A**	(0)	(0)	(0)
conformer **B**		0.1	1.1
TS (*py*,*e*-*ph*)	11.4	7.5	8.7
TS (*py*,*x*-*ph*)	11.4	8.4	8.7
TS (*py*)	12.7	8.4	9.6
TS (*ph*,*ph*)	4.8	13.3	13.9

[a] Corresponding data for the (1-pyrenyl)diphenylmethyl cation (**2**) are included for comparison.

The 1,6- and 1,8-Bis(diphenylmethylenium)pyrene Dications 3 and 4. The dications **3** and **4** are rather large species (196 valence orbitals) and were studied only by the AM1 method. For both compounds, two ground-state minima corresponding to different conformers A and B were located. The stable conformers **3A** and **3B** (C_2 and C_i symmetry) and **4A** and **4B** (C_2 and C_s symmetry) are indicated in Figure 4.

Conformational interconversion around one cation center transforms conformer A into conformer B and vice versa. Conformers **3A** and **3B** have essentially similar energy, but conformer **4A** is predicted to be about 1 kcal/mol more stable than **4B**, probably as a result of slight

Table 4. ^{13}C Chemical Shifts[a] of 2-4Br

compd	*T* (°C)	C-1	C-2	C-3	C-4	C-5	C-6	C-7	C-8	C-9	C-10
2	300	146.5	142.8	127.9	129.9	141.9	135.7	130.8	135.0	136.6	128.4
2	225	144.0	141.8	126.9	128.5	140.4	133.8	129.2	133.0	134.6	127.3
2	205	143.7	141.9	126.8	188.3	140.3	133.6[d]	129.0	132.8[d]	134.4	127.2
2	194	143.5	141.7	126.6	128.2	140.2	133.4	128.9	132.7	134.25	127.1
3	300	141.8[d]	142.2[d]	131.0	134.1	134.3		142.2	131.0	134.1	134.4
3	215	139.8[g]	139.6[g]	129.4	132.3	133.3		139.6	129.4	132.2	133.3
3Br	300	144.9 (br)	139.5	127.4	134.7	132.7	149.9 (br)	139.5	127.4	134.7	132.7
3Br	215	143.1	137.3	125.5	133.8	130.8	143.1	137.3	125.5	133.8	130.8
4	300	143.1	143.3	131.8	137.7	137.7	131.8	143.3	143.1	131.2	131.2
4	215	140.82,[h] 140.74[h]	141.8[k]	130.19, 129.99	136.15, 135.93	136.15, 135.93	130.19	141.8[k]	140.7	129.50, 129.51	129.50, 129.51
4Br	300	140.6	144.7	127.5	130.7	130.7	127.5	144.7[k]	140.6[k]	136.9	136.9
4Br	205	137.99,[i] 137.88	142.00,[i] 142.55	125.64,[i] 125.47	129.20 (br)	129.20 (br)	125.64,[i] 125.47	142.00,[i] 142.55[k]	137.99,[i] 137.88	135.26,[i] 135.04	135.26,[i] 135.04

[a] In ppm. [b] br, broad. [c] Hidden. [d] May be interchanged. [e] Second leg is hidden. [f] May be interchanged. [g] May be interchanged. [h] Two decimals are given so that the separation between the two resonances can be estimated. [i] Are pairwise coalesced at 225 K. [j] Broad but not coalesced at 225 K. [k] Assignment tentative.

steric interference of the two *endo*-phenyl groups in the latter. TS structures for conformational rearrangement around one cation center were estimated assuming idealized geometries as explained above. Calculated relative energies for low-lying TSs are included in Table 3, and the corresponding molecular structures are indicated in Figure 5.

In the (1-pyrenyl)diphenylmethyl monocation system, **2**, two-ring (*ph*,*ph*) flip was clearly predicted as the process with lowest AE, 4.8 kcal/mol; see above. The corresponding TS was predicted to be stabilized by the conjugative effect of the 1-pyrenyl group *py*, which becomes coplanar with the cation center during this process. However, in the dications **3** and **4** the (*ph*,*ph*) rotation process is much less favored, with predicted activation energies between 13 and 14 kcal/mol. The *py* moiety in **3** and **4** carries a diphenylmethylenium substituent and is formally positively charged; stabilization of the (*ph*,*ph*) TS due to the conjugative effect of the *py* group is thus virtually eliminated.

At least three processes in the dication system are predicted with lower activation enthalpy than (*ph*,*ph*), all involving *py* flipping. During these rearrangements, one or both *ph* groups becomes coplanar with the cation center, and conjugation with these formally uncharged groups leads to more efficient TS stabilization. In fact, the activation enthalpies for these processes are predicted to be slightly lower than for the corresponding processes in the monocation **2** (Table 3). The situation is thus predicted to be significantly different for the dication and the monocation systems. For the dications, the lowest activation enthalpies are predicted for (*py*,*ph*) or (*py*) flippings. All dynamic processes considered lead to equilibration of equivalent positions in the pyrene ring systems of the A and B conformers. Moreover, a combination of (*py*,e-*ph*) and (*py*,x-*ph*) processes, which are predicted to have rather similar activation enthalpies (Table 3), lead to equilibration of equivalent positions in the phenyl rings.

NMR Studies. Sample Preparation. The carbenium ions were generated from the corresponding alcohols at dry ice/acetone temperature with FSO_3H/SO_2ClF (a few drops of CD_2Cl_2 served as the NMR lock). The ^{1}H and ^{13}C NMR spectra were recorded between 225 and 194 K. The room-temperature reaction of the alcohols with CF_3COOD produced the same carbocations, which were stable at room temperature. This allowed their NMR study at ambient temperature (300 K) for comparison with the low-temperature spectra.

For all the compounds **2**−**4Br**, the presence of a carbon resonance at ∼200 ppm is clearly indicative of carbenium ion formation, all having a persistent green color.

Assignment of NMR Spectra. The assignments of the ^{13}C NMR spectra are given in Table 4. The assignments are based on chemical shifts of the parent compounds, substituent effects, and HETCOR spectra.[19] For **4** and **4Br** the resonances can be divided into two sets according to intensity, and the more intense is assigned to the lower energy conformation of isomers A (Figure 5). These splittings appear to be very similar in the two spectra and therefore provide a relation between resonances observed in the spectra of **4** and **4Br**.

The assignments of the ^{1}H NMR spectra were based on H,H coupling constants, substituent effects on chemical shifts, and in some cases COSY[20] and HETCOR[19] 2D spectra. Assignment of all the proton resonances belonging to the phenyl rings was in most cases not possible due to severe overlap of resonances. However, some very diagnostic features are visible especially for the low-frequency resonances of H-2′ and H-3′. These resonances are discussed as structural gauges (see later).

(19) Bax, A. *J. Magn. Reson.* **1983**, *53*, 517.
(20) Bax, A.; Freeman, R. *J. Magn. Reson.* **1981**, *44*, 452.

Table 4 (Continued)

C-3a	C-5a	C-8a	C-10a	C-10b	C-10c	C-1′ + C1″	C-2′ + C-2″	C-3′ + C-3″	C-4′ + C-4″	C^+	solvent
144.4	133.5	132.8	139.8	125.7	122.8	~143.3 (br), ~144.1 (br)	142.3 (br), 140.2 (br)	132.8 (br)	141.5 (br)	201.4	CF_3COOD
142.0	131.4	142.0[c]	131.4	126.0	123.2	142.8, 142.1	~141.6, ~139.6	130.9, 130.3	140.0	199.5	SO_2ClF
141.7	131.2	130.7	137.3	125.8	123.0	142.8, ~141.8	142.15, 141.1, 138.9[e]	130.8, 130.2	139.8, 139.7	199.3	SO_2ClF
141.7	131.0	130.4	137.1	125.8	123.0	142.4, 141.7	142.2, 141.0, ~139.7,[c] 138.8	130.6, 130.1	139.7, 139.5	199.1	SO_2ClF
141.5[f]	140.9[f]	141.5	140.9	126.6	126.6	144.8	144.4	133.1	146.2	210.0	CF_3COOD
139.9[g]	139.5[g]	139.9[g]	139.5[g]	124.8	124.8	142.5, 143.3	144.0, 142.3, 142.3, 141.2	131.69, 131.66	144.5	206.9	SO_2ClF
144.9 (br)	139.5[c]	144.9 (br)	139.5[c]	127.1	127.1	144.9 (br)	144.9 (br)	133.4	147.3	n.o.	CF_3COOD
142.1	137.9	142.1	137.9	125.4	125.4	143.1, 143.9	145.6, 143.1, 143.1, 139.3	131.8	145.3	205.9	SO_2ClF
139.7	139.7	141.2	141.2	126.7	126.7	144.8	144.5	133.0	145.9	209.2	CF_3COOD
138.04, 137.53	138.04, 137.53	139.27, 138.99	139.27, 138.99	~124.60, ~124	~124.6, 124	144.23,[c] 143.89,[c] 143.49, 143.31	142.90,[k] 142.69,[k] 142.43,[k] 143.09,[k] 142.97[k]	131.33, 131.22, 130.90	144.54,[k] 144.38,[k] 144.23,[k] 143.89[k]	206.62, 205.17	SO_2ClF
n.o.	n.o.	n.o.	n.o.	127.1	127.1	n.o.	144.7 (br)	130.9	146.9	n.o.	CF_3COOD
139.17,[i] 138.87	139.17,[i] 138.87	136.85,[j] 136.34	136.85,[i] 136.34	125.17,[i] 125.15	125.17,[i] 125.15	144.71, 144.21, 143.98, 143.98	143.26, 143.11, 142.92, 142.55, 142.04, 141.73	131.58,[h] 131.41, 131.12	145.74, 145.44, 145.30, 143.13	206.00, 204.79	SO_2ClF

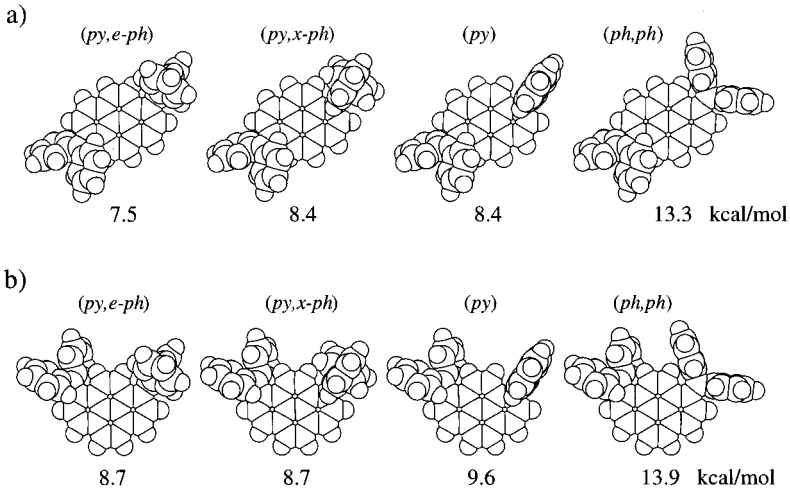

Figure 5. Model transition-state structures for the most favored conformational interconversions (a) of **3A** and **3B** and (b) **4A** and **4B** (AM1 activation enthalpies in kcal/mol).

The greater simplicity of both the ^{13}C and ^1H NMR spectra at ambient temperature helped in the assignment process. Other common useful features are intensities and differential line broadenings.

Spectral Features. At 194 K the ^1H spectrum of **2** exihibits sharp resonances for the pyrene moiety. Some of the ^1H resonances belonging to the phenyl moieties are sharp and some are broad. An interesting feature is the observation of a doublet and a triplet at low frequency, each integrating 2H due to H-2′ and H-3″ of the phenyl moieties (Figure 6a). These resonances broaden at 205 K and move strongly to higher frequency at 225 K.

The ^{13}C spectrum of **2** at 195 K shows sharp pyrene resonances. The resonances for the phenyl rings show two different sharp resonances for C-3′,C-3″. The same is true for C-1′,C-1″ (although one is masked at this temperature) and for C-4′,C-4″. However, C-2′ and C-2″ show two pairs of resonances (Figure 7). The splitting of the pairs are reduced considerably at 225 K. The chemical shift difference of C-3′ and C-3″ is conserved at 225 K, whereas the resonances of C-4′ and C-4″ now coincide. The second resonance of the C-1′,C-1″ pair is now clearly observed.

The ambient-temperature ^1H NMR spectrum of **2** shows sharp resonances for the pyrene moiety. A broad resonance for H-4′,H-4″ and three broad resonances in the approximate ratio 1:2:1 for H-2′, H-2″, H-3′ and H-3″ are shown as well (Figure 6b). The ^{13}C spectrum shows two broad resonances for C-1′,C-1″ and for C-2′,C-2″, whereas the C-3′,C-3″ resonances are close together (Figure 7b).

The ^1H low-temperature spectra of **4** are rather invariable in the temperature range 205−225 K. The H-4,H-5 resonance of pyrene shows two doublets at high frequency. The H-9,H-10 resonances give rise to likewise two singlets at low frequency. In the same manner, the H-2,H-3 and H-6,H-7 resonances are two sets of doublet

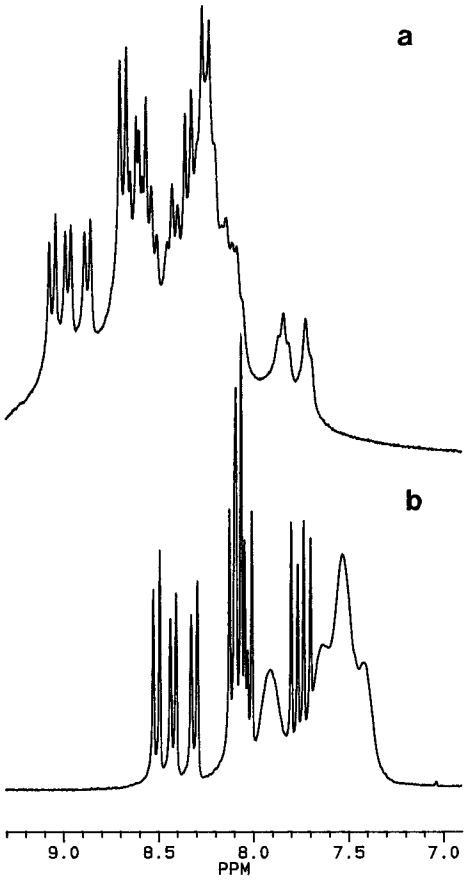

Figure 6. ^{1}H NMR spectra of **2** at (a) 194 K in SO_2ClF and (b) at 300 K in CF_3COOD.

of doublets. The resonances of the phenyl rings show also a characteristic pattern with a low frequency doublet (H-2″) and two low-frequency triplets (H-3′) combined with a large number of unresolved resonances in the middle of the spectrum and two triplets to higher frequency (H-4′ and H-4″) (Figure 8).

All resonances in the ^{13}C spectrum of **4** at 215 K are comparatively sharp and are for the pyrene moiety split into two except for C-4,C-5. The observed splittings are of variable size and as large as 0.5 ppm. The C^+ resonance shows a splitting of 1.45 ppm. Most of the resonances belonging to the phenyl rings appear to be doublets judging from the number of resonances, but considerable overlap makes a detailed analysis difficult. The C-4′, C-4″, C-1′, C-1″, C-2′, C-2″, and C-2,C-7 carbons show 13 separate resonances in the 141.8−144.5 ppm range. The spread is slightly smaller than for **4Br**.

The ^{1}H spectrum of **4** in CF_3COOD at 300 K shows sharp resonances for all protons except H-3′ and H-4′ and no doubling of resonances. The corresponding ^{13}C spectrum shows sharp resonances for all carbon resonances belonging to the pyrene moiety. The C-2′, C-3′, and C-4′ are slightly broadened.

The ^{1}H NMR spectrum of **4Br** at 205−215 K is very similar to that of **4** except that H-2,H-7 is now showing singlets and the H-4,H-5 resonances are shifted to high frequency. At 225 K the ^{1}H spectrum is broadened.

The low-temperature ^{13}C NMR spectrum of **4Br** is very similar to that of **3** except that C-3,C-6 resonances are shifted to low frequency. The C-4′, C-4″, C-1′, C-1″, C-2′, C-2″, and C-2,C-7 carbons show 15 separate resonances between 142 and 146 ppm (Figure 9a). The splittings characteristic for **4** and **4Br** are starting to collapse at 225 K.

In CF_3COOD at ambient temperature the picture is much different for **4Br**. In the ^{1}H spectrum the H-2, H-4, and H-10 resonances of pyrene are sharp and the resonances belonging to the phenyl groups are somewhat broadened, whereas in the ^{13}C spectrum only C-4 and C-10 remain sharp. At 310 K the remaining resonances are even broader.

The low-temperature ^{1}H spectra of **3** at 215 K show a high-frequency doublet with small splittings. The same is found for H-3. Three resonances are outside the main body of resonances, two doublets, one of which shows further splittings (see **3Br**) and a triplet (H-3′) at low frequency.

The ^{13}C spectrum of **3** at 215 K consists of single resonances for all types of pyrene carbons. The phenyl ring carbon resonances are a singlet for C-4, C-4″ and doublets for C-2, C-2″ and for C-3,C-3″ (Figure 9c).

The ambient-temperature (300 K) ^{1}H NMR spectrum of **3** in CF_3COOD shows sharp resonances for all hydrogens belonging to the pyrene moiety and for H-4′,H-4″, whereas those of H-2′,H-2″ and H-3′,H-3″ are broad and close together. No additional splittings of resonances are observed. The ^{13}C spectrum of **3** shows 12 sharp singlets.

In the temperature range 195−215 K the ^{1}H NMR spectrum of **3Br** consists of sharp resonances belonging to the pyrene moiety. The phenyl ring proton part is very similar to that of **3**. At 215 K, the extra splitting of H-4,H-5 had disappeared and that of one of the doublets is about to disappear.

The ^{13}C NMR spectrum of **3Br** is simple as only the C-1′, C-1″ and the C-2′,C-2″ carbon resonances show two resonances at 195 and 215K (Figure 9b).

The ambient-temperature spectra for **3Br** are similar to those of **4Br** in that they only show a few sharp resonances (H-4,H-9 and H-5 and H-10 and the corresponding carbon resonances).

Discussion

On the basis of the NMR spectra at different temperatures, the dynamics of these crowded triaryl compounds can be discussed.

For **2**, the appearance at 195−215 K of four resonances for C-2′, C-2″ shows that the rotation around the C^+−C-1′ and C^+−C-1″ axes is so slow that the C-2′a and C-2′b resonances are different, likewise for C-2″a and C-2″b. The observation of H-2′ doublet (1H) and the H-3′ triplet (1H) resonances at lower frequencies supports this and is a common motif for nonaveraging around the C^+−C-1′ and C^+−C-1″ bonds.

Some averaging has started at 225 K. Now only two resonances are observed for C-2′,C-2″ and two for C-3′,C-3″. For C-4′,C-4″ a coincidence of resonances occurs. However, at this temperature two separate H-4′,H-4″ triplets occur in the ^{1}H spectrum. This shows that the ring is not rotating fast at 225 K. The rotational picture at 225 K is apparently one in which both phenyl rings rotate around the C^+−C-1′ or C^+−C-1″ axis. As demonstrated in the theoretical section, the rotation around the C^+−C-1′ or C^+−C-1″ axis is not sufficient to average the phenyl ring positions. The coalesence point for phenyl ring flipping can be estimated to approxi-

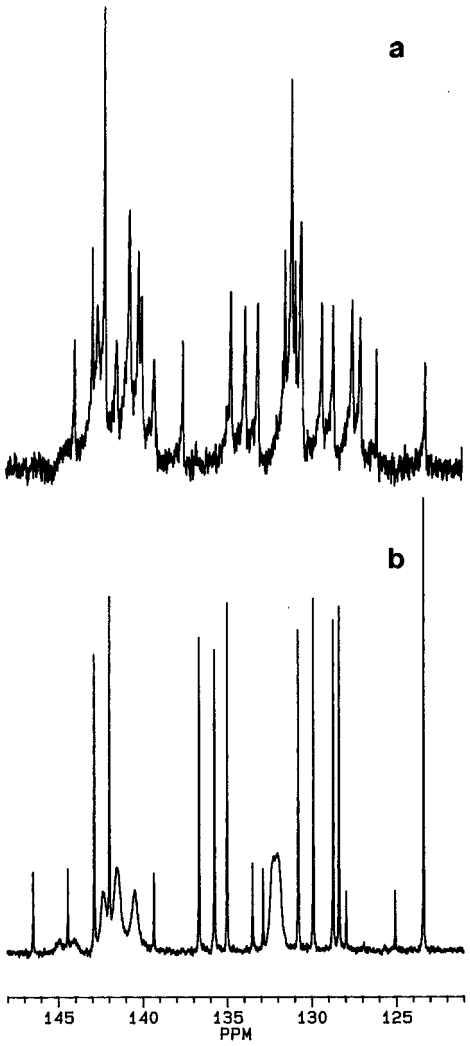

Figure 7. ^{13}C NMR spectra of **2** (a) at 194 K in SO_2ClF and (b) at 300 K in CF_3COOD.

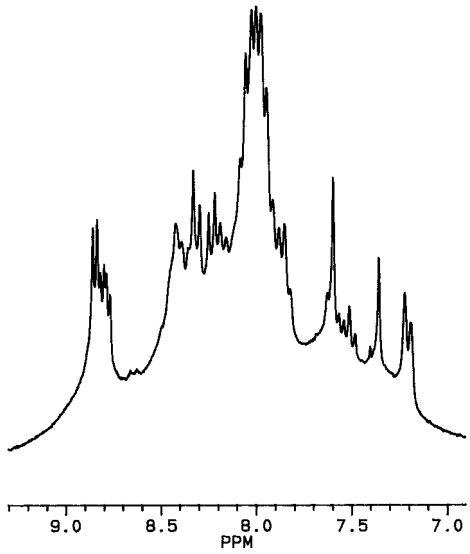

Figure 8. ^{1}H NMR spectra of **4**.

mately 215 K, which gives an activation energy of less than 40 kJ/mol (10 kcal/mol).

At 300 K the pyrenyl ring is also rotating, but not fast enough to fully average C-3′ and C-3″ or C-2′ and C-2″.

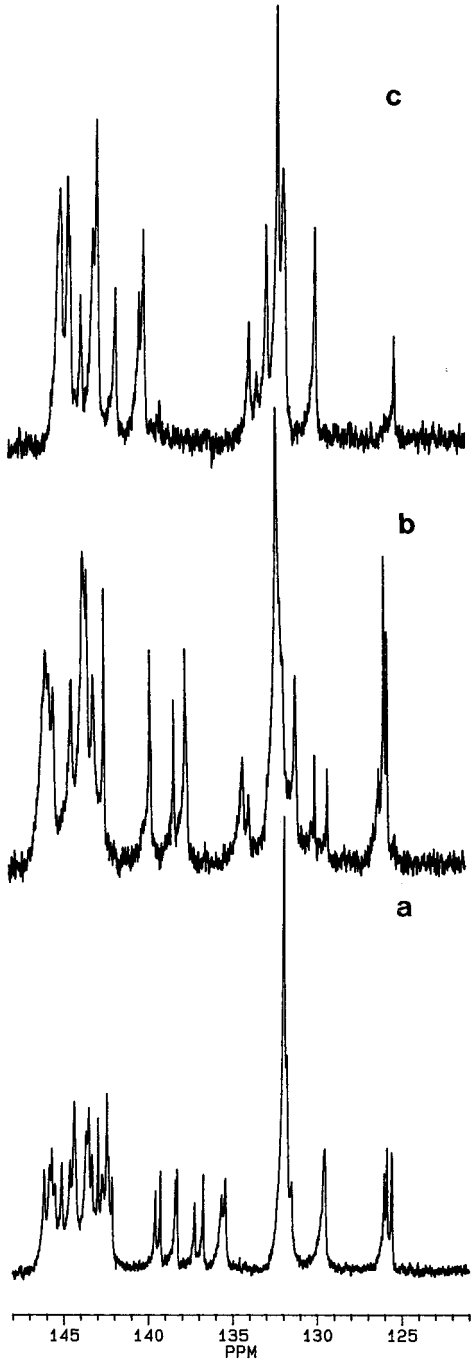

Figure 9. ^{13}C NMR spectrum of (a) **4Br**, (b) **3Br**, and (c) **3**.

The rotational picture for **4** at 215 K is different from that of **2**. The interesting observation is the occurrence of two sets of resonances in a ca. 1:1 ratio. These two sets can be explained by the existence of two different isomers, **4A** and **4B** (Figure 5). The rotational barrier is high enough to prevent averaging of these two species at low temperature, and the phenyl rings are close enough to interfere with each other. At ambient temperature, averaging takes place and only resonances corresponding to one species are found. The pyrenyl ring rotation is not sufficiently fast to give sharp resonances for H-2′,H-2″ and for H-3′,H-3″ at ambient temperature.

The low-temperature spectra for **4Br** at 205 K are very similar to those of **4**, but at 225 K some rotation occurs to average the pairs of resonances. However, the low-frequency motif mentioned for **2** occurred in the same

Table 5. ^{1}H C-hemical Shifts and ^3J(H,H) of 2-4Br in CF_3COOD at 300 K

	H-2	H-3	H-4	H-5	H-6	H-7	H-8	H-9	H-10	H-2′	H-3′	H-4′	H-2″	H-3″	H-4″
2	7.78	8.10	8.10	8.51	8.42	8.06	8.31	8.02	7.71	7.42	7.63	7.90	7.53	7.53	7.90
a	8.63			8.71	7.58		7.75		9.27	vbr[b]	br[b]	br	br	br	br
3	8.11	8.53	8.25	7.93		8.11	8.53	8.25	7.93	∼7.8	7.88	8.30	∼7.8	7.47	8.17
a	8.30	8.33	9.24	9.32		8.30	8.33	9.24	9.32	vbr	vbr	7.27, 7.32	vbr	vbr	7.27, 7.37
3Br	8.29		8.61	7.84		8.29		8.61	7.84	7.85	7.85	8.29	7.85	7.85	8.29
a	br		br	br		br		br	br	br	br	br	br	br	br
4	8.20	8.70	8.75	8.75	8.70	8.20		7.46	7.46	∼7.7	7.84	8.27	∼7.7	7.84	8.27
a	8.36	8.30	s	s	8.30	8.36		s	s	vbr	br	7.36, 7.42	vbr	br	7.36, 7.42
4br	8.40		9.23	9.23		8.40		7.42	7.42	7.68	7.80	8.26	7.68	7.80	8.26
a	s		s	s		s		s	s	br	br	br	br	br	br

[a] Coupling constants. [b] br, broad; vbr, very broad. [c] s, singlet.

position, indicating that the rotation of the phenyl rings is slow. The ambient temperature spectra of **4Br** are for most resonances broad for unknown reasons.

The low-temperature spectra of **3** at 215 K are in many respects similar to those of **4** except that no doubling of resonances is seen in the ^{13}C spectrum. For **3** and **3Br** only small splittings are observed in the ^{1}H spectra at low temperature. These splittings disappear at higher temperature. Both compounds can exist in forms with C_2 and C_i symmetry (Figure 5). As the substituents are far away from each other, the interference is minimal and the ring conformations are very similar in the A and B isomer. This combined with a lower rotational barrier (see Table 3) makes the observation of the two species difficult. That the geometry of the three compounds **2**−**4** indeed are slightly different is seen from the positions of the H-2′ and H-3′ chemical shifts (Table 5).

The ambient temperature spectra of **3** show features identical to those of **4**.

For **3Br**, the low-temperature spectra are very similar to those of **3**. The ^{13}C spectrum of **3Br**, which is by far the most simple of all spectra, shows two separate resonances for C-2′ but not for C-2″ (they may be interchanged). The resonances for C-1′,C-1″ have merged into a broad resonance and so have the resonances of C-4′,C-4″ (Figure 9b). This pattern is not consistent with a two-ring (*ph*,*ph*) flip but is in line with a two-ring (*py*,*ph*) flip.

At ambient temperature, all the carbocations except for **2** show only a single resonance for the phenyl ring resonances (C-1′,C-1″, C-2′,C-2″, C-3′,C-3″ and C-4′,C-4″) showing that averaging around the C$^+$−C-1 bond in **2** is fast. As judged from the theoretical calculations, this can be either one-ring (*py*) flip or more likely due to two-ring (*py*,*ph*) flips.

By a comparison of the merging of lines with equal separation, a comparison of activation energies can be made in the compounds **2**−**4**. The activation energy is largest for **3** and **4** followed closely by **3Br** and **4Br** and the disubstituted ones are higher in energy than **2** in agreement with calculations for **2**−**3** and **4** (Table 3).

Charge Distributions. The chemical shift values for the C$^+$ carbons are indicative of the degree of charge delocalization. The calculations indicate that this should be the largest for **2**. This can also be inferred from the ^{13}C chemical shifts. The C$^+$ chemical shifts for **3**, **3Br**, **4** and **4Br** are slightly lower than that found for **1** underlining the large capacity of the pyrenyl ring for charge delocalization. This is furthermore seen for the aromatic carbons as the calculated charge differences between the carbenium ion and the parent alcohol, Δq_C's, show that extensive charge delocalization occurs into both the pyrenyl and phenyl rings in an alternating fashion. For **3** and **4** the picture is in general similar taking into consideration the different positions of the substituents.

A comparison of the charge distribution in **3A** and **3B** shows very little difference between the two species, whereas a comparison of the charges of **4A** and **4B** reveals small differences that in most cases are proportional to the splittings for the pyrenyl resonances of **4** and **4Br**. However, this is not so for the C$^+$ carbons as the C$^+$ resonances are separated in the former case by 1.45 ppm and in the latter by 1.23 ppm and the charge difference is as small as 0.0015.

Experimental Section

Synthesis of the Precursor Alcohols. The crowded mono- and diols were prepared from the corresponding mono- and dibenzoyl derivatives of pyrene (or its dibromopyrene) by reaction with PhLi. The benzoyl derivatives were prepared by conventional Friedel−Crafts-type benzoylation of pyrene (or its dibromo derivative). The synthetic details have been previously published.[21]

FSO_3H (Fluorochem or Aldrich) was doubly distilled in an all-glass distillation unit and stored in Nalgene bottles. SO_2ClF (high purity grade) was purchased from Aldrich in glass ampules, stored in a Schlenk tube in the freezer, and used without further purification.

Stable Ion Generation and NMR. The procedure for stable ion generation in FSO_3H/SO_2ClF was analogous to our previously reported methods.[22]

The ions prepared at ambient temperature were made by mixing with CF_3COOD.

The NMR spectra were recorded on a Bruker-250 MHz or a GE-GN-300 MHz instrument. CD_2Cl_2 served as both internal lock and reference for the low-temperature measurements. For details see ref 22. At ambient temperature in CF_3COOD, the CF_3 resonance served as reference.

NMR Data of Starting Carbinols. ^{1}H NMR ($CDCl_3$). **2**: δ 3.45 (s, 1H) OH; 7.43 (d, J = 8.25, 1H) H-2; 7.85 (d, J = 9.55, 1H) H-9; 7.94 (d, J = 7.5, 1H) H-6; 7.97 (d, J = 7.80, 1H) H-8; 7.96 (br, 1H) H-3; 7.96 + 8.00 (m, 2H) H-4 + H-5; 8.13 (m, 1H) H-7.

3: δ 3.70 (s, 1H) OH; 7.33 (m, 20H) H-2′,H-3′,H-4′; 7.42 (d, J = 8.3, 2H) H-2,H-7; 7.81 (d, J = 9.4, 2H) H-4,H-9; 7.90 (d, J = 8.1, 2H) H-3, H-8; 8.41 (J = 9.3, 2H) H-5, H-10.

3Br: δ 3.79 (s, 2H) OH; 8.32 (m, 20H) H-2′,H-3′,H-4′; 7.80 (s, 2H) H-2,H-7; 8.22 (d, J = 10.0, 2H) H-4,H-9; 8.49 (d, J = 9.6, 2H) H-5, H-10.

4: 3.39 (s,2H) OH; 7.32 (m, 20H) H-2′,H-3′H-4′; 7.37, (d, J = 8.1, 2H) H-2, H-7; 7.93 (d, J = 8.1, 2H) H-3,H-6; 7.97 (s, 2H) H-4,H-5; 8.21 (s, 2H) H-9,H-10.

4BR: 3.35 (s, 2H) OH; 7.30 (m, 20H) H-2′,H-3′,H-4′; 7.71 (s, 2H) H-2,H-7; 8.19 (s, 2H) H-9,H-10; 8.50 (s, 2H) H-4,H-5.

^{13}C NMR ($CDCl_3$). **2**: 83.73, COH; 123.60, C-10; 124.78, C-10c; 125.28, C-8; 125.32, C-6; 126.03, C-3; 126.78, C-7; 126.97, C-2; 127.31, C-9; 127.36, C-4′, 127.70, C-5; 127.87, C-4;

(21) Lund, H.; Berg, A. *Kgl. Videnskab. Selskab* **1941**, *18*, 1.
(22) Laali, K. K.; Hansen, P. E. *J. Org. Chem.* **1991**, *56*, 6795.

127.95, C-3′, 128.11, C-2′; 129.53, C-10a; 130.33, C-5a; 131.26, C-8a; 140.02, C-1; 142.61, C-1′.

3: 83.72, COH; 123.11, C-10b; 123.75, C-2; 125.55, C-3; 127.00, C-5; 127.18, C-4′; 127.83, C-3′, 128.01, C-2′, 130.40, C-10a; 130.76, C-3a; 139.47, C-1; 147.39, C-1′.

3Br: 83.38,OH; 120.40, C-3; 125.43, C-5; 126.83, C-10b; 127.72, C-4′; 127.85, C-3′; 128.36, C-2′; 128.84, C-4; 129.14, C-3a; 129.19, C-10a, 132.42, C-2; 141.62, C-1; 146.65, C-1′.

4: 83.70, COH; 123.28, C-9; 126.00, C-10b; 126.28, C-2′; 127.80, C-4′; 127.89, C-3′; 127.93, C-3; 127.99, C-4; 128.08, C-2′; 128.70, C-8a; 131.5, C-3a; 140.33, C-1; 147.42, C-1′.

4Br: 83.26, COH; 119.84, C-3; 126.24, C-9; 126.85, C-10b; 127.53, C-4′; 127.67, C-3′; 127.85, C-4; 128.19, C-2′; 128.42, C-8a; 129.62, C-3a; 132.54, C-2; 141.73, C-1; 146.49, C-1′.

Acknowledgment. We are grateful to the NCI of NIH (R15CA63595 to K.K.L.) and to NATO (CRG 930113 to K.K.L. and P.E.H.) for research support in the PAH arenium ions area. We would also like to thank Professor A. Berg for donating the carbinols.

JO9715480